

Extinction imaging of a single quantum emitter in its bright and dark states

P. Kukura, M. Celebrano[†], A. Renn, and V. Sandoghdar*

Laboratory of Physical Chemistry and optETH, ETH Zurich, CH-8093 Zurich, Switzerland

[†]*Permanent address: Department of Physics, Politecnico di Milano, 20133 Milan, Italy*

Room temperature detection of single quantum emitters has had a broad impact in fields ranging from biophysics [1, 2] to material science [3], photophysics [4], or even quantum optics [5]. These experiments have exclusively relied on the efficient detection of fluorescence. An attractive alternative would be to employ direct absorption, or more correctly expressed “extinction” [6] measurements. Indeed, small nanoparticles have been successfully detected using this scheme in reflection [7, 8, 9] and transmission [10, 11]. Coherent extinction detection of single emitters has also been reported at cryogenic temperatures [12, 13, 14, 15], but their room temperature implementation has remained a great laboratory challenge owing to the expected weak signal-to-noise ratio [16]. Here we report the first extinction study of a single quantum emitter at ambient condition. We obtain a direct measure for the extinction cross section of a single semiconductor nanocrystal both during and in the absence of fluorescence, for example in the photobleached state or during blinking off-times [17]. Our measurements pave the way for the detection and absorption spectroscopy of single molecules or clusters of atoms even in the quenched state.

Ensembles of emitters, such as atoms, molecules, ions, or quantum dots, are routinely studied via absorption or fluorescence spectroscopy alike. However, conventional absorption spectroscopy is difficult to perform on very dilute samples because one has to detect very small changes on a large signal. For a dye molecule placed in a diffraction-limited laser spot, a simple estimate predicts an extinction dip of about 2×10^{-6} if we consider a typical cross section of $\sigma \sim 1 \times 10^{-15} \text{ cm}^2$ at room temperature. In this letter we demonstrate that a direct extinction measurement can be nevertheless successful in detecting a single quantum emitter without using any noise suppression methods such as lock-in detection. We performed our experiments on semiconductor nanocrystals, which have been shown to behave like artificial atoms with well-defined quantized energy levels and nonclassical emission photon statistics [5]. We chose such nanocrystal quantum dots (NQD) because they have slightly larger absorption cross sections than dye molecules and last much longer than these before photobleaching [18].

The schematics of our experimental setup is depicted

in Fig. 1a and described in the Methods section. Here it suffices to state that we illuminate the sample with a focused laser beam at a wavelength of 532 nm and detect the fluorescence and the reflected excitation light on separate detectors. Images are produced by raster scanning the sample. We examined various commercially available NQDs with ensemble extinction spectra shown in Fig. 1b. The NQDs were spin cast on freshly cleaved thin mica sheets that are known to yield locally atomically flat surfaces [19]. This was important for minimizing the fluctuating background that one encounters when employing the scheme of Fig. 1a on a standard microscope cover glass [20].

Figures 2a and b show examples of simultaneously recorded fluorescence and reflection images of a sample prepared using D2 NQDs. The observed intermittent fluorescence in (a) proves that the signal stems from a single NQD [4]. Fig. 2c displays this more clearly by a time trace of the fluorescence signal recorded from the NQD under constant illumination. The on-off blinking behavior of fluorescence is illustrated further in Fig. 2e by a histogram of the fluorescence counts, yielding two well defined peaks. Thus, Fig. 2b presents an image of a single quantum emitter recorded in reflection with a signal contrast of about 6×10^{-4} . This is substantially larger than the estimate we stated earlier. We now explain the origin of this enhanced signal and relate it to the extinction cross section of a NQD.

In a transmission experiment, the signal I_{det} on the

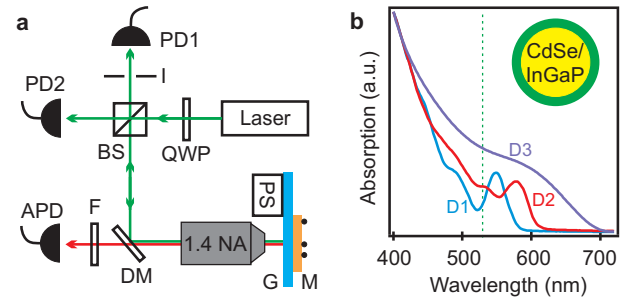


FIG. 1: Setup. (a) Schematics of the optical system and sample arrangement. PD1: photodiode for detection of the extinction signal; PD2: photodiode for normalization of the laser intensity; I: Iris; BS: 50:50 beam splitter; QWP: quarter wave plate; DM: dichroic mirror; F: long pass filter; APD: avalanche photodiode; G: microscope cover glass slip; M: mica sheet; PS: piezo scanner. (b) Ensemble extinction spectra of the nanocrystal quantum dots used in this work. Details are provided in the Methods section. The curves are scaled to match at the short wavelength end.

*Electronic address: vahid.sandoghdar@ethz.ch

detector can be obtained by writing [6]

$$I_{\text{det}} = |\mathbf{E}_{\text{exc}} + \mathbf{E}_{\text{sca}}|^2 = |\mathbf{E}_{\text{exc}}|^2 + |\mathbf{E}_{\text{sca}}|^2 + 2\text{Re}[\mathbf{E}_{\text{exc}}^* \mathbf{E}_{\text{sca}}]. \quad (1)$$

where \mathbf{E}_{exc} denotes the complex electric field of the excitation beam. The field \mathbf{E}_{sca} scattered by the sample is given by $\mathbf{E}_{\text{sca}} \propto |\alpha|e^{i\phi_{\text{sca}}}\mathbf{E}_{\text{exc}}$ where α is the complex polarizability of the particle, and ϕ_{sca} is the scattering phase shift determined by the real and imaginary parts of α . The last term in Eq. (1) is known as the “extinction signal” and signifies the interference between \mathbf{E}_{exc} and \mathbf{E}_{sca} . For small particles it is much larger than the second term and can be expressed as the sum of the absorption and scattering cross sections [6]. In reflection, \mathbf{E}_{exc} is replaced by $r\mathbf{E}_{\text{exc}}$ where r is the sample reflectivity. Hence, the signal contrast is increased by $r^{-1} \sim 5$ for the mica/air interface [7]. Measurements in reflection or transmission are otherwise equivalent because in each case the scattered light interferes with the excitation beam. Therefore, we refer to our signal obtained in reflection also as the extinction signal.

A second mechanism for enhancing the extinction signal in our experiment stems from the optimization of the phase difference between \mathbf{E}_{exc} and \mathbf{E}_{sca} . The symbols in Fig. 2d show the measured variation in the extinction signal of a NQD as a function of its displacement from the focus. This strong position dependence is caused by the change in the phase $\phi_{\text{exc}} - \phi_{\text{sca}}$ where ϕ_{exc} denotes

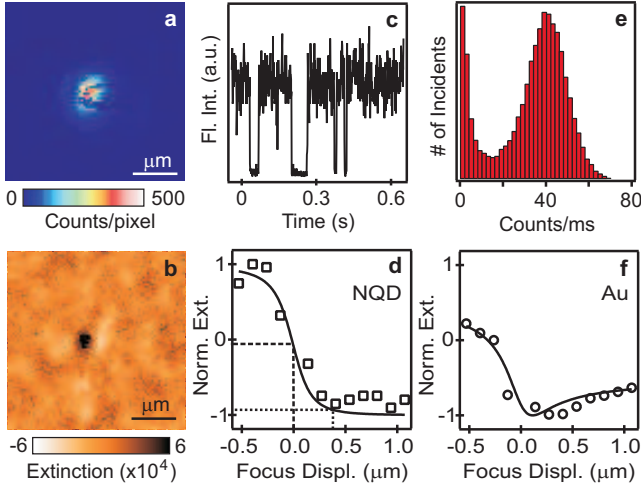


FIG. 2: Extinction detection of a single quantum dot (a) A fluorescence image of an individual D2 quantum dot (excitation intensity of 2 kW/cm^2). (b) Corresponding extinction image (6 averages). (c) Partial fluorescence trajectory of the dot in (a) (time bin: 1 ms, excitation intensity 200 W/cm^2). (d) The normalized variation of the extinction signal of a D3 type NQD as a function of its displacement from the focus along the optical axis (symbols: experimental; line: theoretical). Here we chose D3 dots because their large σ provided reliable signals even away from the maximum. (e) Histogram of fluorescence counts collected from the dot in (a) over 50 s. (f) Same as in (d) but for a single gold nanoparticle with a diameter of 10 nm.

the phase of the focused laser beam dictated by the Gouy phase [21]. The solid line plots a theoretical fit. Details are provided in the Methods section. This data reveal that the extinction signal is enhanced by roughly ten times if one moves away from the focus by $+400 \text{ nm}$. Indeed, in each run we optimized the signal by displacing the sample.

Obtaining a value for the extinction cross section based on the measured contrast is not an easy matter because we do not have a quantitative knowledge of the mode overlap between \mathbf{E}_{exc} and \mathbf{E}_{sca} [14]. To remedy this difficulty, we chose to compare the signal contrast obtained from a NQD with that of a gold nanoparticle (GNP) of diameter 10 nm, which has a well-known extinction cross section [6]. We prepared a sample containing both GNPs and NQDs and imaged them under identical conditions, yielding an extinction contrast of 3.5×10^{-3} for a single GNP. As shown by the symbols in Fig. 2f, the extinction signal of a GNP does not vary substantially within a displacement of $+400 \text{ nm}$ from the focus.

By comparing the in-focus extinction contrasts of 3.5×10^{-3} and 6×10^{-5} for GNPs and NQDs respectively, and taking the literature value of $\sigma_{\text{Au}} = 2.7 \times 10^{-13} \text{ cm}^2$ [11], we arrive at $\sigma_{\text{NQD}} = 4.5 \times 10^{-15} \text{ cm}^2$. This value is in good agreement with $2 \times 10^{-15} \text{ cm}^2$ obtained from ensemble extinction measurements [22] and $3 \times 10^{-15} \text{ cm}^2$ extracted from fluorescence studies of similar sized single NQDs [23]. This level of agreement between our measured values of extinction contrast and the expected extinction cross sections holds for all three quantum dots in Fig. 1b. However, we emphasize that we observe a substantial spread of up to 3 times in the extinction signals recorded from different individual NQDs of nominally the same type. Furthermore, as reported previously [24], we also find no stringent correlation between the extinction and fluorescence signals of individual dots.

In addition to pushing the limits of optical imaging, fluorescence-free detection of emitters provides important insight into their complex photophysical properties such as photobleaching and fluorescence blinking. Figures 3a and b depict fluorescence and extinction images obtained from averaging 6 individual scans. Subsequent to the acquisition of these images, the marked dot was selectively irradiated with an elevated intensity until it was photo-bleached and no further fluorescence was observed. The same area as in (a) and (b) was then scanned to obtain images (d) and (e), respectively. A comparison of Figs. 3b with e and examination of Fig. 3c show that aside from the marked NQD all image features are reproduced in (e). In fact, it turns out that the marked dot is also faintly visible in the extinction image (e) although it is completely absent in the fluorescence signal (d). Figure 3f displays cuts from Figs. 3b and e, revealing a three-fold drop in the extinction cross section of the NQD. This finding is consistent with the hypothesis that the NQD polarizability might be decreased as a consequence of photo-oxidation [18]. These results establish the first report on the interrogation of a single emitter

after its quantum transitions were irreversibly modified.

The most fascinating photophysical property of NQDs is their fluorescence blinking [17], and many groups have studied this effect by analyzing the fluorescence signal [23, 25, 26, 27]. We now show that our detection mechanism makes it possible to examine the system even in the absence of fluorescence, i.e. in the blinking off-state. Following the procedure described earlier, we first identified a single NQD and then repeatedly scanned it through the laser beam along one line to record both its fluorescence and extinction data. Next, we summed the total fluorescence counts for each line and plotted the outcome for 2500 lines. As shown in Fig. 4a, this yields a familiar blinking trace. By setting lower and upper thresholds shown by the horizontal lines, we isolated line scans in which the NQD was clearly in the off and on states. The data selected in this fashion were averaged to arrive at the fluorescence and extinction line scans shown in Figs. 4b and c, respectively. While there is roughly a 10-fold difference in the fluorescence intensity between the on and off states, no difference in the extinction signal can be observed. We also repeated the same experiment with D1 NQDs (see Fig. 1b), which show longer off-times. Consequently, as plotted in Fig. 4e, the contrast in fluorescence between the on and off states is now much stronger. Nevertheless, Fig. 4f shows that again the extinction signals of the on and off states remain identical. We thus conclude that within the accuracy of our measurement, the room temperature extinction cross section of a NQD does not change upon blinking.

Although a theoretical treatment of the extinction cross section away from a sharp resonance is not straightforward [22], we can gain insight into some of its funda-

mental features by considering the cross section of a two-level quantum system given by $\sigma = \frac{3\lambda^2}{2\pi} \frac{\gamma_{\text{rad}}}{\gamma_{\text{hom}}}$ [28]. Here λ is the transition wavelength, and γ_{rad} and γ_{hom} denote the radiative and homogeneous linewidths respectively, whereby $\gamma_{\text{hom}} > \gamma_{\text{rad}}$ by 4-5 orders of magnitude at room temperature. Thus the lack of change in the extinction signal of NQDs indicates that most likely, neither of λ , γ_{rad} , and γ_{hom} has been modified between the on and off states. In other words, the NQD has not undergone a transition to a new quantum state. Instead, we believe our observation is consistent with models where the fluorescence is quenched in the off state by fast nonradiative relaxation of the excited state [26, 29]. To illustrate this, we point out that $\gamma_{\text{hom}} = \sum \gamma_i$ with γ_i signifying various contributions to line broadening. Hence, if a nonradiative quenching rate $\gamma_q \ll \gamma_{\text{hom}}$ is activated, its influence on σ remains negligible while it crucially diminishes the fluorescence quantum efficiency $\eta = \frac{\gamma_{\text{rad}}}{\gamma_{\text{rad}} + \gamma_q}$.

The unprecedented detection sensitivity of the extinction measurements reported in this letter can be improved even further by several measures. First, the residual optical roughness of the sample, evident in the comparison of Figs. 3b, e, and c, can be eliminated. In addition, where applicable techniques such as polarization modulation can help discriminate against such background fluctuations. Thus, given that the extinction cross section of a NQD is only a few times larger than that of conventional dye molecules, extinction detection of these should be also within reach. In particular, emitters

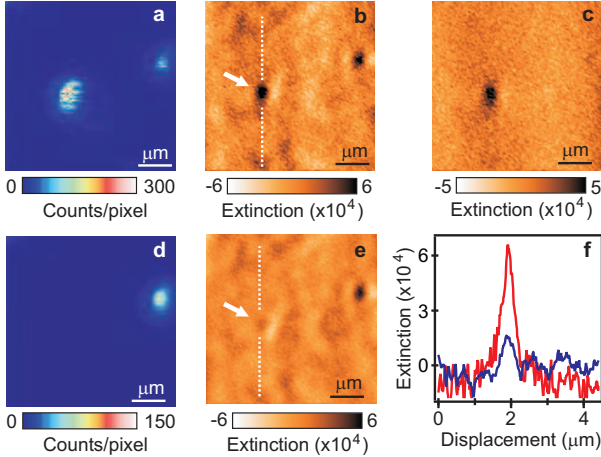


FIG. 3: **Photobleaching study** Fluorescence (a) and extinction (b) images of two individual D2 quantum dots. The marked dot was the same as the one studied in Fig. 2. (c) Difference between images (b) and (e). (d,e) Images obtained after illuminating the marked NQD with 20 kW/cm² for several minutes. (f) Cross section of the quantum dot before (red) and after (blue) photobleaching.

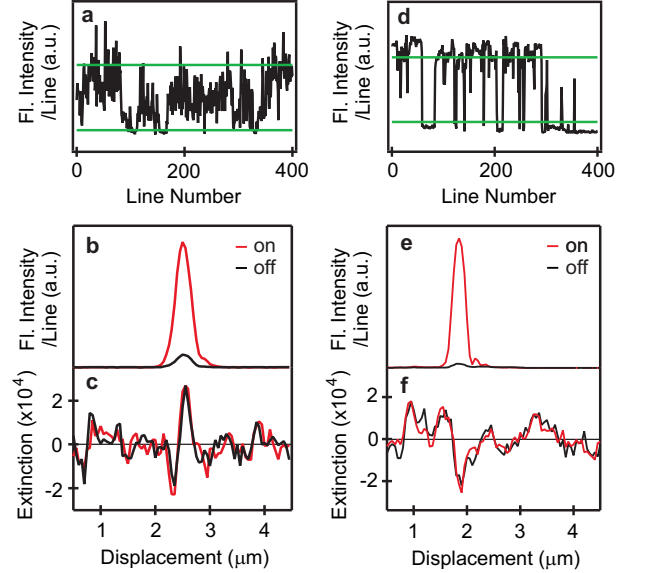


FIG. 4: **Blinking study** (a) Sum of fluorescence counts obtained from one-dimensional line scans across a single D2 NQD for 400 lines. The green lines indicate boundaries where the dot is determined to be on or off. (b) Resulting fluorescence cross sections after averaging about 100 lines that lie below and above the indicated thresholds. (c) Corresponding extinction line scans. (d-f) Same as (a-c) but for a D1 NQD.

with quenched fluorescence, for example close to metallic surfaces or in chemical contact [30], are not disadvantaged in extinction measurements and become accessible to optical investigations. Furthermore, by employing white light confocal microscopy [7], it should be possible to record extinction spectra of individual nanoparticles and molecules in an efficient manner. These techniques provide exciting opportunities for extending the applicability of nano-optical studies to a much wider range

of material and environments than has been available to fluorescence measurements.

The authors thank J. Hwang, M. Agio, N. Mojarad, and G. Zumofen for discussions and S. Walt for help with the investigation of mica surfaces. This work was supported by the ETH Zurich, Swiss National Foundation (SNF) and the Swiss Ministry of Education and Science (EU Integrated Project Molecular Imaging).

-
- [1] Betzig, E. *et al.* Imaging intracellular fluorescent proteins at nanometer resolution. *Science* **313**, 1642–1645 (2006).
 - [2] Michalet, X. *et al.* Quantum dots for live cells, in vivo imaging, and diagnostics. *Science* **307**, 538–544 (2005).
 - [3] Kirstein, J. *et al.* Exploration of nanostructured channel systems with single-molecule probes. *Nature Mat.* **6**, 303–310 (2007).
 - [4] Dickson, R. M., Cubitt, A. B., Tsien, R. Y. & Moerner, W. E. On/off blinking and switching behaviour of single molecules of green fluorescent protein. *Nature* **388**, 355–358 (1997).
 - [5] Michler, P. *et al.* A quantum dot single photon turnstile device. *Science* **290**, 2282 (2000).
 - [6] Bohren, C. F. & Huffman, D. R. *Absorption and Scattering of Light by Small Particles* (John Wiley and Sons, 1983).
 - [7] Lindfors, K., Kalkbrenner, T., Stoller, P. & Sandoghdar, V. Detection and spectroscopy of gold nanoparticle using supercontinuum white light confocal microscopy. *Phys. Rev. Lett.* **93**, 037401–1 (2004).
 - [8] Ignatovich, F. V. & Novotny, L. Real-time and background-free detection of nanoscale particles. *Phys. Rev. Lett.* **96**, 013901 (2006).
 - [9] Ewers, H. *et al.* Label-free optical detection and tracking of single virions bound to their receptor in supported membrane bilayers. *Nano Lett.* **7**, 2263–2266 (2007).
 - [10] Mikhailovsky, A. A., Petruska, M. A., Stockman, M. I. & Klimov, V. I. Broadband near-field interference spectroscopy of metal nanoparticles using a femtosecond white-light continuum. *Opt. Lett.* **28**, 1686–1688 (2003).
 - [11] Arbouet, A. *et al.* Direct measurement of the single-metal-cluster optical absorption. *Phys. Rev. Lett.* **93**, 127401 (2004).
 - [12] Plakhotnik, T. & Palm, V. Interferometric signatures of single molecules. *Phys. Rev. Lett.* **87**, 183602 (2001).
 - [13] Karrai, K. & Warburton, R. J. Optical transmission and reflection spectroscopy of single quantum dots. *Superlattices and Microstructures* **33**, 311–337 (2003).
 - [14] Gerhardt, I. *et al.* Strong extinction of a laser beam by a single molecule. *Phys. Rev. Lett.* **98**, 033601 (2007).
 - [15] Wrigge, G., Gerhardt, I., Hwang, J., Zumofen, G. & Sandoghdar, V. Efficient coupling of photons to a single molecule and the observation of its resonance fluorescence. *Nature Phys.* **4**, 60–66 (2008).
 - [16] Hwang, J., Fejer, M. M. & Moerner, W. E. Scanning interferometric microscopy for the detection of ultrasmall phase shifts in condensed matter. *Phys. Rev. A* **73**, 021802(R) (2006).
 - [17] Nirmal, M. *et al.* Fluorescence intermittency in single cadmium selenide nanocrystals. *Nature* **383**, 802–804 (1996).
 - [18] Peng, X., Schlamp, M. C., Kadavanich, A. V. & Alivisatos, A. P. Epitaxial growth of highly luminescent cdse/cds core/shell nanocrystals with photostability and electronic accessibility. *J. Am. Chem. Soc.* **119**, 7019–7029 (1997).
 - [19] Hegner, M., Wagner, P. & Semenza, G. Ultralarge atomically flat template-stripped au surfaces for scanning probe microscopy. *Surf. Sci.* **291**, 39–46 (1993).
 - [20] Jacobsen, V., Stoller, P., Brunner, C., Vogel, V. & Sandoghdar, V. Interferometric optical detection and tracking of very small gold nanoparticles at a water-glass interface. *Opt. Express* **14**, 405–414 (2006).
 - [21] Hwang, J. & Moerner, W. E. Interferometry of a single nanoparticle using the gouy phase of a focused laser beam. *Opt. Comm.* **280**, 487–491 (2007).
 - [22] Leatherdale, C. A., Woo, W.-K., Mikulec, F. V. & Bawendi, M. G. On the absorption cross section of cdse nanocrystal quantum dots. *J. Phys. Chem. B* **106**, 7619–7622 (2002).
 - [23] Kuno, M., Fromm, D. P., Hamann, H. F., Gallagher, A. & Nesbitt, D. J. "on"/"off" fluorescence intermittency of single semiconductor quantum dots. *J. Chem. Phys.* **115**, 1028–1040 (2001).
 - [24] Berciaud, S., Cognet, L., Blab, G. A. & Lounis, B. Photothermal heterodyne imaging of individual nonfluorescent nanoclusters and nanocrystals. *Phys. Rev. Lett.* **93**, 257402 (2004).
 - [25] Verberk, R. & Orrit, M. Photon statistics in the fluorescence of single molecules and nanocrystals: Correlation functions versus distributions of on- and off-times. *J. Chem. Phys.* **119**, 2214–2222 (2003).
 - [26] Fisher, B., Eisler, H., Stott, N. & Bawendi, M. Emission intensity dependence and single-exponential behavior in single colloidal quantum dot fluorescence lifetimes. *J. Phys. Chem. B* **108**, 143–148 (2004).
 - [27] Pelton, M., Smith, G., Scherer, N. F. & Marcus, R. A. Evidence for a diffusion-controlled mechanism for fluorescence blinking of colloidal quantum dots. *Proc. Natl. Acad. Sci. USA* **104**, 14249–14254 (2007).
 - [28] Loudon, R. *Quantum Theory of Light* (Oxford University Press, 2000).
 - [29] Frantsuzov, P. A. & Marcus, R. A. Explanation of quantum dot blinking without the long-lived trap hypothesis. *Phys. Rev. B* **72**, 155321 (2005).
 - [30] Lakowicz, J. R. *Principles of Fluorescence Spectroscopy* (Kluwer Academic, Plenum Publishers, New York, Second Edition, 1999).

Methods

The output of a low noise diode-pumped solid-state laser at 532 nm is spatially filtered, expanded by a 5:1 telescope, circularly polarized and split by a 50:50 beam splitter. One half of the light is sent to a home-built inverted microscope and focused onto the sample with a high numerical aperture microscope objective (Zeiss Apochromat, 1.4 NA, 63x). The fluorescence is separated from the excitation light by a dichroic mirror and a long pass filter before it is detected by an avalanche photodiode (APD) in the photon counting mode. The extinction signal is sent through a confocal pinhole and then a photodiode (PD1) coupled to a low noise current to voltage amplifier. An iris is used to remove the component of the excitation light that underwent total internal reflection at the substrate/air interface. A second amplified photodiode (PD2) monitors the laser intensity.

Fluorescence and extinction images were acquired by raster scanning the sample across the focus with a x-y piezo translation stage. By normalizing and subtracting the signals on both photodiodes, laser intensity fluctuations are reduced by roughly an order of magnitude to about 0.01% RMS after normalization. Rapid scanning aided in reducing noise due to slow drifts in the objective/sample distance and laser pointing fluctuations.

We used commercially available PEG coated core/shell quantum dots with emission centered at 565 nm (D1: Invitrogen, Qdot 565 ITK amino (PEG), CdSe/ZnS), 600 nm (D2: Evident Technologies, EviTags E2-C11-CB2-0600, CdSe/ZnS) and 680 nm (D3: Evident Technologies,

EviTags E2-C11-NF2-0680, InGaP/ZnS). The stock solutions were diluted 10000-fold before spin casting 10 μ L of the diluted solution onto the sample substrate at 3000 rpm for 30 seconds.

We used freshly cleaved mica sheets as substrate to minimize background fluctuations in the extinction signal [20]. To avoid complications in the imaging caused by the substrate birefringence, we produced sheets less than 1 μ m thick. These were adhered to standard microscope cover glass with a small drop of immersion oil for index matching. The sample was immediately placed on a spin coater and rotated at 3000 rpm for 30 seconds to remove any excess oil.

The scattering phase ϕ_{sca} can be obtained using the textbook expression for α [6] and the complex refractive indices of the material of the particle under study. We used the literature values for the complex refractive index of the various materials (E. D. Palik, Handbook of Optical Constants of Solids, (Academic Press, Boston 1985)), as well as an average refractive index of 1.31 for the mica/air interface to arrive at scattering phases $\phi_{\text{Au}} = 0.26\pi$, $\phi_{\text{CdSe}} = 0.06\pi$ and $\phi_{\text{InGaP}} = 0.015\pi$. If we approximate the focused laser beam as a Gaussian beam, its Gouy phase variation is given by $\phi_{\text{exc}} = \tan^{-1}(\lambda z / \pi w_0^2)$, where z is the displacement from the focus, and w_0 is the half beam waist. The z-coordinate of the focus was determined by fitting the fluorescence spot to a Gaussian and locating the position at which the full width at half maximum is minimized.